Stem Cell Research & Therapy

RESEARCH

Open Access

Combination of rapamycin and adipose-derived mesenchymal stromal cells enhances therapeutic potential for osteoarthritis

Damien Veret[1,2], Gautier Tejedor[2], Esther Perez[2], Alison Chomette[2], Maylis Farno[2], Rosanna Ferreira-Lopez[1,3,4], Louis Dagneaux[5], Yves-Marie Pers[1,3], Christian Jorgensen[1,3], Claire Gondeau[2†] and Jean-Marc Brondello[1*†]

Abstract

Background The regenerative potential of mesenchymal stromal/stem cells (MSCs) has been extensively studied in clinical trials in the past decade. However, despite the promising regenerative properties documented in preclinical studies, for instance in osteoarthritis (OA), the therapeutic translation of these results in patients has not been fully conclusive. One factor contributing to this therapeutic barrier could be the presence of senescent cells in OA joints.

Methods This study evaluated a novel approach to OA treatment by combining adipose tissue-derived MSCs (AD-MSCs) with rapamycin, a clinically approved immunosuppressive drug with anti-senescence properties. First, rapamycin effects on senescence and fibrosis markers were investigated in freshly isolated OA chondrocytes by immunostaining. Next, the in vitro differentiation capacities of AD-MSCs, their regulatory immune functions on activated immune cells and their regenerative effects on OA chondrocyte signature were assessed in the presence of rapamycin.

Results In OA chondrocytes, rapamycin reduced the senescence marker $p15^{INK4B}$ and the fibrosis marker COL1A1 without affecting the expression of the master chondrogenic markers SOX9 and COL2. Rapamycin also enhanced AD-MSC differentiation into chondrocytes and reduced their differentiation into adipocytes. In addition, rapamycin improved AD-MSC immunoregulatory functions by promoting the expression of immunosuppressive factors, such as *IDO1*, *PTGS2* and also *CD274* (encoding PD-L1). Finally, RNA sequencing analysis showed that in the presence of rapamycin, AD-MSCs displayed improved chondroprotective regenerative effects on co-cultured OA chondrocytes.

Conclusions Our findings suggest that the rapamycin and AD-MSC combination enhances the therapeutic efficacy of these cells in senescence-driven degenerative diseases such as OA, notably by improving their anti-fibrotic and anti-inflammatory properties.

Keywords Mesenchymal stromal/stem cells, Rapamycin, Regenerative medicine, Osteoarthritis

† Claire Gondeau and Jean-Marc Brondello are co-authorships.

*Correspondence:
Jean-Marc Brondello
jean-marc.brondello@inserm.fr
Full list of author information is available at the end of the article

Graphical abstract

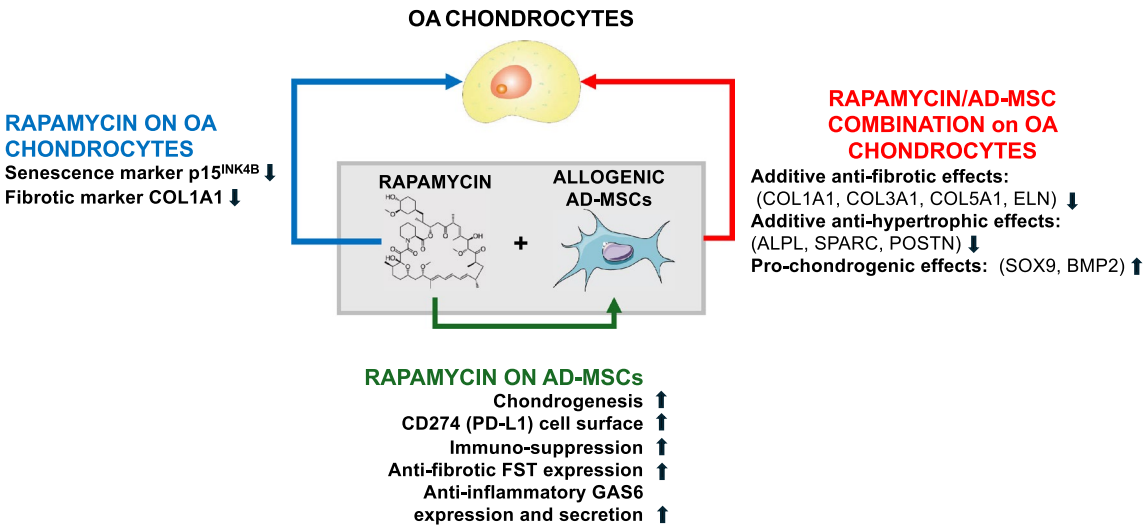

Introduction

Mesenchymal stromal/stem cells (MSCs) are the most widely described multipotent stem cells in regenerative medicine [1, 2]. They can be isolated mainly from adipose tissue (so called AD-MSCs) [3], bone marrow [4], or umbilical cord [5]. They display many interesting features, especially the ability to expand while maintaining their stemness and the potential to differentiate in vitro and in vivo into chondrocytes, adipocytes and osteoblasts [6]. In an inflammatory microenvironment and through unique paracrine and juxtacrine mechanisms, MSCs also display immunoregulatory properties by suppressing the activation of immune cells or changing their phenotypes toward pro-regenerative functions [7]. Therefore, in the last decades, MSCs have been tested as regenerative therapeutics in many diseases, including ischemia, chronic wound healing conditions and osteoarthritis (OA) ([8] for review).

OA is a rheumatic disease for which there is no effective treatment [9]. It is characterized by the loss of joint homeostasis, leading to fibrotic degenerated cartilage, inflamed synovium and subchondral bone remodeling. It is now thought that OA is caused by the accumulation of senescent articular cells [10]. One proposed etiologic mechanism is based on the concomitant dysregulation of the pro-fibrotic and pro-senescent TGF-β signaling pathway and hyperactivation of the mTOR-AKT axis, both observed in OA chondrocytes from pre-clinical models and human samples [11].

Based on the in vitro MSC regenerative potential and success in preclinical OA studies, clinical trials have been conducted by us [12] and others to test the effect of intra-articular infusions of in vitro-amplified MSCs in the degenerated joints of patients with OA. However, a recent systematic review and meta-analysis on MSC effectiveness for chronic knee pain secondary to OA (807 patients enrolled in 16 randomized trials) [13] showed that intra-articular injection of MSCs leads to little or no improvement in pain and physical function. Therefore, to overcome the limitations of primary MSCs, preconditioning strategies (for instance, with clinically approved pharmacological molecules) or genetic modification are now tested to enhance their functionality [14].

Rapamycin (sirolimus) is a lipophilic antibiotic derived from *Streptomyces hygroscopicus* and belongs to the macrolide family having immunosuppressive properties, which also includes ciclosporin and tacrolimus ([15] for review). Thus, it is an approved anti-proliferative and immunosuppressive drug mainly prescribed to prevent transplant rejection by graft-versus-host disease [15]. Rapamycin binds to FKBP12 and thus, interacts with and then inhibits the mTOR pathway, impairing protein synthesis while improving autophagic flux [16]. Rapamycin also reduces the cytokine storm in patients with COVID-19 and antibody production by B lymphocytes [15]. Moreover, preclinical studies showed that in senescent cells, rapamycin is an effective senotherapeutic drug [17].

In this study, we assessed whether the combination of rapamycin and AD-MSCs, produced following Good Manufacturing Practices (GMP) standards in media supplemented with human platelet lysat (HPL) [18], could be more effective to treat senescence-driven OA cartilage

degeneration. To this aim, we evaluated the in vitro rapamycin beneficial effects on AD-MSC differentiation potential, immunosuppressive functions and regenerative capacities to restore functionality of chondrocytes isolated from OA patients.

Materials and methods

Media and reagents

Dulbecco's minimal essential medium (DMEM) and trypsin–EDTA were purchased from Biowest. Minimal essential medium alpha (MEM-α), Iscove's modified Dulbecco's medium (IMDM), HEPES, non-essential amino acids solution (NEAA), sodium pyruvate, β-mercaptoethanol, insulin-transferrin-selenium (ITS + 2), fetal bovine serum (FBS), and TrypLE™ select were from Gibco. L-glutamine, penicillin–streptomycin (P/S), and phosphate-buffered saline (PBS) were from Corning. Human platelet lysate Stemulate® (HPL) was from Sexton Biotechnologies, Cryostor® CS10 from BioLife Solutions, and interferon gamma (IFN-γ) from Biotechne. Collagenase II, Pronase E, cell culture-grade DMSO, methanol-free paraformaldehyde (PFA), bovine serum albumin (BSA), Triton X-100, Tween-20, dexamethasone, ascorbate 2-phosphate, proline, phytohemagglutinin (PHA) were from Sigma. Rapamycin was from Merck. The MesenCult™ ACF Chondrogenic Differentiation Kit, MesenCult™ Osteogenic Differentiation Kit (Human), and MesenCult™ Adipogenic Differentiation Kit (Human) were from STEMCELL™. CellTrace™ Violet, LIVE/DEAD™ Fixable Near-IR, and Hoechst 33,342 were purchased from ThermoFisher.

Antibodies

The anti-SOX9 mouse monoclonal antibody, clone GMPR9 (1:200), anti-collagen II mouse monoclonal antibody, clone 2B1.5 (1:200), goat anti-rabbit IgG (H + L) highly cross-adsorbed secondary antibody, Alexa Fluor™ 647 (1:500) and goat anti-mouse IgG (H + L) cross-adsorbed secondary antibody, Alexa Fluor™ 488 (1:500) were purchased from ThermoFisher. The anti-CDKN2B rabbit polyclonal antibody (orb213719, 1:200) was from Biorbyt and the anti-COL1A1 XP® rabbit monoclonal antibody (E8F4L, 1:500) and anti-PPAR-γ rabbit monoclonal antibody (C26H12, 1:400) were from Cell Signaling. The APC-coupled anti-human CD274 (B7-H1, 1:100) antibody was from BioLegend.

Human adipose-derived stromal cell isolation, expansion and treatment

Human AD-MSCs were isolated from abdominal adipose tissue obtained from four healthy adults after they signed an informed consent, as previously described [19]. The donors' body mass index ranged from 24.7 to 30.0. AD-MSC production was standardized to comply with the GMP. Cells were expanded twice in Quantum hollow-fiber bioreactors (Terumo BCT) in MEMα containing 5% HPL and were characterized as MSCs according to the ISCT recommendations. AD-MSCs were frozen in Cryostor® CS10 at passage 1 (P1). For experiments, cells were thawed and resuspended in MEMα, 5% HPL, 1% P/S. For amplification, AD-MSCs (4.5×10^3 cells/cm^2) were seeded in flasks and maintained at 37 °C in the same medium for 4 days. For IFN-γ stimulation, AD-MSCs (4 donors) were seeded at 1.5×10^4 cells/cm^2 in 6-well plates for 24 h before incubation with 20 ng/mL IFN-γ in the presence of 10 nM rapamycin or 0.01% DMSO (control). After 48 h, cells were processed for RNA sequencing or flow cytometry analysis.

Human chondrocytes isolation and culture

Human OA chondrocytes were isolated as previously described by Malaise *et coll.* [20], from cartilage obtained from patients with OA who underwent total knee arthroplasty at Lapeyronie hospital, France, after obtaining their informed consent. Briefly, cartilage from the tibial plate and condyles was removed and cut into small pieces. The recovered cartilage samples were weighed, washed twice with DMEM, 1% P/S, 1% L-glutamine, and digested with Pronase E (50 µg/mL) in the same medium for 1 h. Then, cartilage samples (5 g per digestion at most) were washed twice and digested with collagenase II (2 mg/mL-10 mL) in the same medium overnight. The next day, samples were neutralized with 1 volume DMEM, 10% FBS, 1% P/S, 1% L-glutamine and passed through a 70 µm sieve. Cell suspensions were centrifuged at 300 g for 5 min, washed once, plated (4,000 cells/cm^2) and expanded twice.

Colony-forming units (CFUs)

AD-MSCs (3 donors) were seeded (100 cells per well) in 6-well plates in triplicate (9.6 cm^2 ~ 10 cells/cm^2) in MEMα, 5% HPL, 1% P/S. The next day, 10,000X stock solution of rapamycin (in DMSO) was diluted 1/10 in medium and added (1/1000) to the wells. Medium was not changed during the 10 days of culture. Then, cell colonies were fixed with ice-cold methanol for 5 min, washed once with water, and stained with 2% Giemsa solution for 10 min with agitation. Cells were washed three times with water and dried. CFUs were counted manually.

Reverse-transcription and quantitative polymerase chain reaction (RT-qPCR)

RT was performed using M-MLV Reverse Transcriptase, a Random Hexamer (both from Invitrogen™) and 250 ng of RNA at the final concentration of 12.5 ng/

µL. The resulting cDNA was diluted five times (2.5 ng/µL) for qPCR analysis that was performed using 5 ng (2 µL) cDNA, the LightCycler® 480 SYBR Green I Master (Roche) and a Roche LightCycler® 480 Instrument II (384-well plates). The primer sequences are in Table S1.

AD-MSC differentiation into chondrocytes, adipocytes and osteoblasts

For adipogenesis and osteogenesis, P1 AD-MSCs (4 donors) were thawed, seeded (4.5×10^3 cells/cm^2) in MEMα, 5% HPL, 1% P/S. Cells were plated in 24-well, 6-well and black 96-well half surface plates for Oil Red O staining (adipogenesis), Alizarin Red staining (osteogenesis), RT-qPCR and immunofluorescence analysis, respectively. After 4 days (cells at 95% of confluence), medium was removed and replaced with the reagents from the Mesencult™ Osteogenic or Adipogenic Differentiation Kit (STEMCELL) in the presence of 10 nM rapamycin or 0.01% DMSO (control). Osteogenic differentiation was evaluated after 10 days (adipo) and 14 days (osteo). Analysis by RT-qPCR, Oil Red O and Alizarin Red staining were then performed (see Supplementary data for details). For chondrogenesis, AD-MSCs (5×10^5 cells from 3 donors) were differentiated in 3D conditions in the presence of the Mesencult™ chondrogenic medium. with/without 10 nM rapamycin. After 21 days, cartilage pellets were lysed for chondrogenic marker quantification by RT-qPCR or stained with Alcian blue.

Immunosuppression assay

Peripheral blood mononuclear cells (PBMCs) from three healthy donors (buffy coats from the Etablissement Français du Sang) were isolated using the Ficoll procedure, pooled and cryopreserved in DMSO supplemented with 10% FBS. Immunosuppression assays were performed by co-culturing AD-MSCs (4 donors) with activated PBMCs at different ratios, as previously described [19] (see Supplementary data for details). To evaluate AD-MSC inhibitory effect on PBMC proliferation, the percentage of PBMC proliferation in co-culture was compared to the proliferation of PHA-activated PBMC alone (set to 100%). The difference between conditions represents the percentage of inhibition.

ELISA analysis of GAS6 secretion by AD-MSCs

GAS6 secretion by AD-MSCs was assessed using the Human GAS6 ELISA Kit (Invitrogen – BMS2291) following the manufacturer's instruction, but by initially diluting samples five times in diluent buffer (see Supplementary data for details).

AD-MSC and chondrocyte transwell co-cultures

To mimic the physiological conditions of intra-articular injection of AD-MSCs, 5×10^5 OA chondrocytes (3 donors) were seeded into wells of 6-well plates with/without 7.2×10^4 AD-MSCs (3 donors) on inserts as previously described [21]. Before co-culture, chondrocytes and AD-MSCs were grown alone for 24 h. For co-culture, medium was replaced with minimal chondrogenic medium (DMEM, 1% P/S, 1% L-glutamine, 1 mM sodium pyruvate, 50 mg/mL ascorbate 2-phosphate, 40 mg/mL proline, 1% ITS + 2, 100 nM dexamethasone) in the presence of 10 nM rapamycin or 0.01% DMSO for 3 days. Total RNA was extracted for RNA sequencing analysis.

Immunofluorescence (IF) staining

For IF analyses, cells were plated in black 96-well plates with half-area well and µclear® bottom (Greiner Bio-One). Cells were fixed with 3.6% PFA/PBS for 30 min, washed twice with PBS and stored at 4 °C for less than 1 week. Before staining, cells were washed once with PBS, permeabilized with PBS/3% BSA/0.3% Triton X-100 for 3 min, washed twice and incubated with a solution containing PBS, 3% BSA, 0.05% Tween-20 for 30 min. Then, cells were incubated with two primary antibody pairs (SOX9/p15^{INK4B} and COL1A1/COL2 for chondrocytes) diluted in PBS/3% BSA/0.05% Tween-20 at room temperature in humidified chambers for 4 h. After two washes with PBS/0.05% Tween-20, cells were incubated with secondary antibodies diluted in PBS/3% BSA/0.05% Tween-20 at 37 °C for 1 h, washed twice with PBS/0.05% Tween-20, and incubated with Hoechst 33,342 (2 µg/mL) in PBS for 5 min. After washing once with PBS, a 90% glycerol-PBS solution was used as mounting medium. A Leica TCS SP8 confocal microscope with LAS X navigator mode and motorized stage was used for image acquisition.

Flow cytometry analysis

AD-MSCs were trypsinized using TrypLE™ Select, incubated with 250 ng of APC-coupled anti-CD274 (PD-L1) antibody or APC-coupled isotype on ice, in the dark for 30 min. Then, cells were washed twice with PBS/1% BSA and resuspend in 500 µL of this buffer before analysis with a FACS Canto II flow cytometer (BD Biosciences). PD-L1 expression in AD-MSCs was quantified with Kaluza Analysis 2.1. The inhibitory effect of AD-MSCs on PBMC proliferation was quantified with the FlowJo software (FlowJo, Ashland, OR, USA).

RNA preparation and sequencing

Total RNA was isolated from AD-MSCs or OA chondrocytes using the RNeasy Mini kit (Qiagen) according

to the manufacturer's instructions. The RNA Integrity Number was evaluated on Agilent chips and for all samples it was > 9. Libraries were prepared by BGI Genomics (Hong Kong, China) using 500 ng of total RNA and the MGIEasy RNA Library Prep Kit (MGI, China). Library quality was assessed on a Bioanalyzer 2100 (Agilent) and quantity by qPCR. The final libraries were formatted as single-stranded circular DNA. Libraries were sequenced on a DNBSEQ G400 sequencer (MGI, China) (paired-end 150) and at least 30 M clean reads were obtained for each library.

RNA sequencing data analysis

RNA sequences were aligned using HiSAT2 to the reference human genome. Differentially expressed genes (DEGs) were identified with the Deseq2 R package. Results were considered significant when Q-value < 0.05. To obtain a reference genome-wide signature from RNA sequencing data of healthy chondrocytes, published data from Fisch *et coll.* [22] on chondrocytes isolated from cartilage samples of 18 healthy donors and 20 patients with OA were used. The raw count table from GSE114007 was retrieved for the Gene Expression Omnibus databank and analyzed using the EdgeR package. A preselection threshold of at least 380 total counts per row (at least 10 counts per sample) was applied. All genes with FDR ≤ 0.05 without log2(FC) thresholding were selected. Heatmaps and volcano plots were generated with the Complex Heatmap and Enhanced Volcano packages, respectively. The list of all OA dysregulated genes was submitted to the *KEGG Pathways* and *REACTOME* databases to identify pathways that were significantly affected in OA. Then, the lists of upregulated and downregulated gene underwent the same process to identify upregulated/downregulated genes in the affected pathways. Pathways significantly affected by OA and the number of "hit" genes were extracted and transferred to GraphPad to be displayed as a double-sided histogram. Then, to identify markers associated with OA physiopathology and senescence, normalized counts of these genes were extracted, converted to log10(Norm.count + 1) and plotted using GraphPad. Similarly, cytokines and growth factors deregulated in OA were identified.

Statistical analysis

All data are presented as median or mean ± SEM. Results from multiple conditions were compared by two-way ANOVA. The Mann–Whitney Student's *t*-test was used for comparisons between two experimental groups. Data were analyzed using the Prism software v10 (GraphPad Software Inc.). *P* values < 0.05 were considered significant ($^{*}p < 0.05$; $^{**}p < 0.01$; $^{***}p < 0.001$).

Results

Rapamycin effects on AD-MSC self-renewal properties and on chondrogenic and pathogenic marker expression in OA chondrocytes

In this study, we wanted to test whether AD-MSC therapeutic potentials could be improved by the concomitant delivery of rapamycin in OA joints. First, we determined whether rapamycin negatively affects AD-MSC self-renewal capacities to form individual colonies. To this end, we seeded AD-MSCs at low density and incubated them with increasing concentrations of rapamycin (10, 50 and 100 nM). After 10 days, we stained cells with Giemsa, counted the number of colonies and found that rapamycin did not affect AD-MSC colony formation at the tested concentrations (Fig. S1A).

We then determined the rapamycin concentration that reduces the expression of OA-associated senescence/fibrosis markers in chondrocytes without affecting the expression of functional chondrogenic markers. To this end, we cultured freshly digested and non-amplified chondrocytes from OA cartilage (from 6 donors) for 1 week and incubated them with 10, 50 and 100 nM rapamycin (or DMSO) for 48 h. Quantification by indirect immunofluorescence staining using antibodies against two chondrogenic markers (SOX9 and COL2) and two OA markers (COL1A1 for fibrosis and TGFβ-induced $p15^{INK4B}$ for senescence) (Fig. 1A and C) showed that rapamycin reduced significantly, and in a dose-dependent manner, the relative expression of $p15^{INK4B}$. Indeed, compared to DMSO, we found a Fold change = 0.82 for 10 nM (meaning 18% of inhibition on its expression level), a Fold change = 0.78 for 50 nM (22% of inhibition) and a Fold change = 0.71 for 100 nM (29% of inhibition) respectively (Fig. 1B). Similarly, we found an inhibition of the relative expression COL1A1 compared to DMSO of 18%

(See figure on next page.)

Fig. 1 Rapamycin anti-fibrotic and anti-senescent effects in primary OA chondrocytes. Primary chondrocytes were isolated from OA cartilage samples (n = 6 donors), cultured at 1.5×10^5 cells/cm^2 (nearly confluent state) for 7 to 10 days in FBS-containing medium, passaged and re-plated (1.5×10^4 cells/cm^2), and 24 h later incubated with 10, 50 or 100 nM rapamycin or 0.01% DMSO (vehicle) for 48 h. **A** Confocal microscopy images and **B** quantification of SOX9 and p15 ^{INK4B} co-staining in OA chondrocytes. **C** Confocal microscopy images and **D** quantification of COL2 and COL1A1 co-staining in OA chondrocytes. Data were plotted and analyzed with GraphPad Prism 10.2.3; *p*-values: * < 0.05, ** < 0.01, *** < 0.001 (two-way ANOVA)

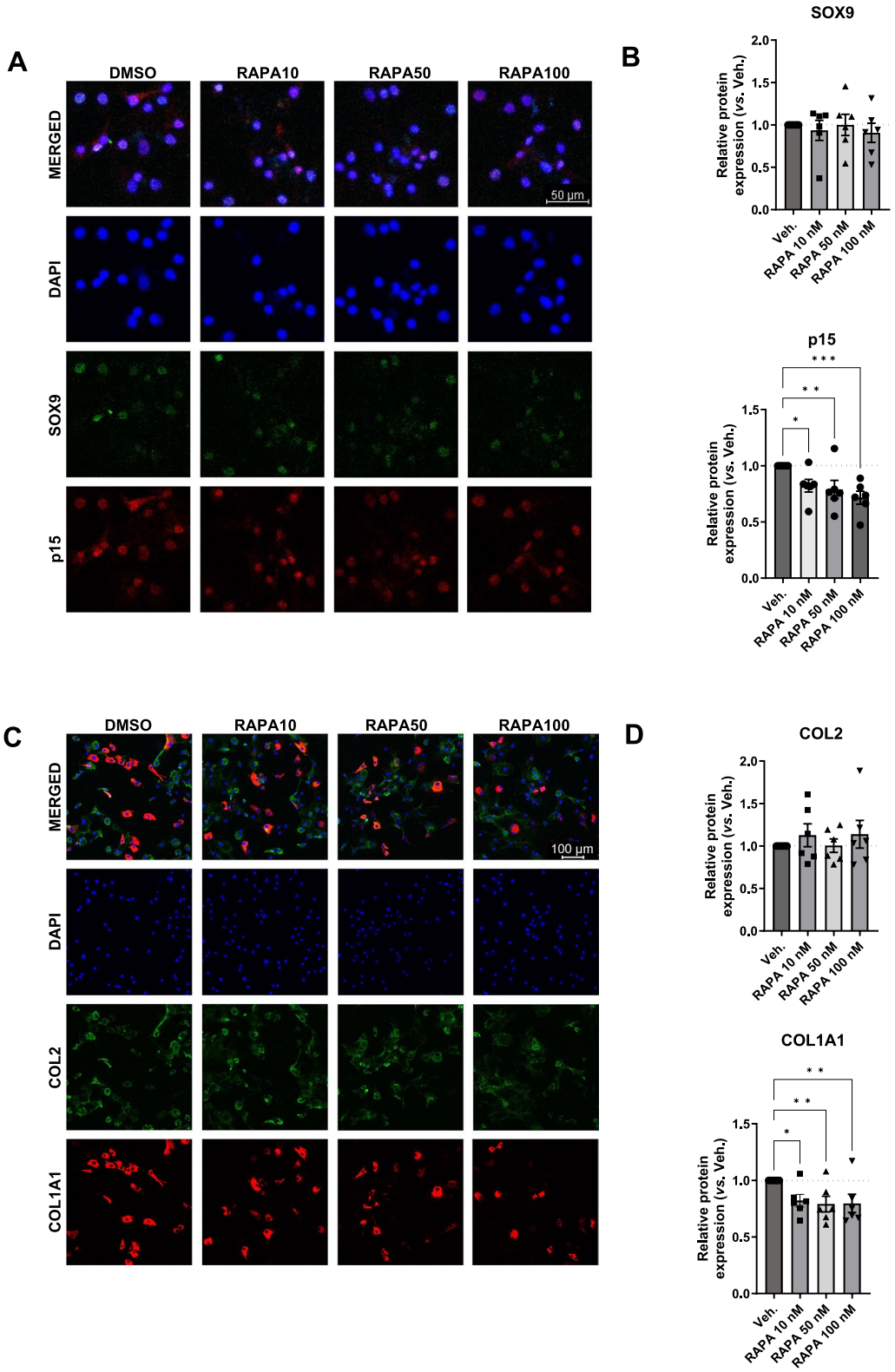

Fig. 1 (See legend on previous page.)

(Fold change = 0.82 for 10 nM), 21% (Fold change = 0.79 for 50 nM) and 21% (Fold change = 0.79 for 100 nM), respectively (Fig. 1D). Conversely, the relative expression of SOX9 (Fig. 1B) and COL2 (Fig. 1D) were not impacted. These data indicate that rapamycin has no negative impact on AD-MSC clonal capacities, but exerts positive effects on OA chondrocytes by reducing the expression of fibrotic and senescence markers. For the next experiments, we used 10 nM rapamycin (*i.e.* the lowest tested concentration).

Rapamycin improves AD-MSC chondrogenic potential and reduces their adipogenic potential

AD-MSCs are adipose tissue-derived MSCs that can differentiate in vitro into adipocytes, osteoblasts or chondrocytes. Therefore, we evaluated rapamycin effect on AD-MSC differentiation compared with DMSO (vehicle). During differentiation into adipocytes (Fig. 2A–B), incubation with rapamycin (10 nM for 2 days) significantly reduced lipid accumulation, quantified by Oil-Red-O staining, in both undifferentiated and differentiated AD-MSCs (Relative staining = 0.79, 1.52 and 1.28 for undifferentiated vehicle, differentiated vehicle and differentiated RAPA, respectively). Conversely, rapamycin did not alter the percentage of PPAR-γ-expressing cells evaluated by immunostaining (Fig. S2A) and the gene expression of the adipogenic markers *PPARG2*, *FABP4*, *LEPTIN* and *ADIPOG* (RT-qPCR) (Fig. S2B).

During differentiation into osteoblasts, rapamycin (10 nM for 2 days) did not alter the mineralization level, quantified by Alizarin Red staining, in newly differentiated bone cells (Fig. 2C–D) and the gene expression of the osteogenic markers *RUNX2*, *SP7*, and *ALP* (RT-qPCR) (Fig. S2C).

Lastly, during chondrogenic differentiation, rapamycin (10 nM for 2 days) did not alter cartilage pellet formation as revealed by Alcian blue staining (Fig. 2E), but increased the gene expression of the chondrogenic markers *SOX9* ($Log_{10}(FC) = 0.23$ with vehicle and 0.59 with rapamycin), and *ACAN* ($Log_{10}(FC) = 0.80$ with vehicle and 1.23 with rapamycin) (Fig. 2F–G).

These results indicate that in AD-MSCs, rapamycin selectively enhances chondrogenic markers and impairs lipid accumulation during adipogenesis, without affecting their capacity to differentiate into bone cells. These findings are in favor of using rapamycin in combination with AD-MSCs for the treatment of osteo-articular diseases, such as OA.

Rapamycin increases AD-MSC immunomodulatory properties

AD-MSCs are primarily used for cell-based regenerative therapy because they can suppress activated immune cell proliferation in an inflammatory context [7]. Indeed, in response to IFN-γ, AD-MSCs express immunoregulatory genes, including *IDO1*, *PTGS2* which encodes COX2 implicated in PGE2 production, and *CD274* which encodes the immune checkpoint regulator PD-L1 [23]. All these factors contribute to reduce or convert the immune cell phenotypes toward anti-inflammatory profiles. To verify whether rapamycin could improve the immunosuppressive functions of IFN-γ-stimulated AD-MSCs, we used RNA sequencing to compare unstimulated AD-MSCs incubated with 0.01% DMSO (vehicle) and IFN-γ-stimulated AD-MSCs incubated or not with 10 nM rapamycin.

IFN-γ stimulation of AD-MSCs alone led to the identification of 2365 DEGs (971 downregulated and 1394 upregulated), some of which were strongly upregulated, including *IDO1* and *CD274* (Volcano plot in Fig. 3A). As expected, gene ontology analysis of the upregulated genes using *REACTOME* identified the IFN-γ signaling and immunity-related pathways (Fig. S3A). Then, we looked at the impact of rapamycin on the genes upregulated by IFN-γ stimulation. We found that 81 genes were upregulated by both IFN-γ and IFN-γ + RAPA (Fig. 3B and heatmap in Fig. 3C). Analysis of these 81 genes with *REACTOME* indicated that they are mainly involved in IFN-γ signaling, immune-related and cytokine signaling pathways, and also in the complement cascade (Fig. S3B). Among these 81 genes, we found that in IFN-γ stimulated AD-MSCs, *IDO1* and *PTGS2* were further upregulated after incubation with rapamycin (Fig. 3D–E). Conversely, *CD274*, which encodes PD-L1 that acts as a "don't kill me" immune checkpoint signal, was upregulated following IFN-γ stimulation ($Log_2(FC) = 4.85$ in

(See figure on next page.)

Fig. 2 Rapamycin effect on AD-MSC differentiation. AD-MSCs at passage 1 were seeded at 4.5×10^3 cells/cm^2 and grown for 4 days before induction of differentiation using STEMCELL Mesencult™ kits. Cells were exposed to 10 nM rapamycin or 0.01% DMSO (vehicle) during the first two days of differentiation. Adipogenesis (n = 4) was stopped after 10 days, osteogenesis (n = 4) after 14 days, and chondrogenesis (n = 3) after 21 days. **A** Adipogenesis visualization by Oil Red O staining. **B** Quantification of Oil Red O staining by measuring the absorbance at 540 nm. **C** Osteogenesis visualization by Alizarin red staining and **D** quantification by measuring the absorbance at 540 nm. **E** Chondrogenic pellets stained with alcian blue. **F**–**G** Relative quantification of the expression of *SOX9* and *ACAN* (cartilage markers) by RT-qPCR in chondrogenic pellets. All error bars represent SEM; *p*-values * < 0.05, ** < 0.01, *** < 0.001 (two-way ANOVA)

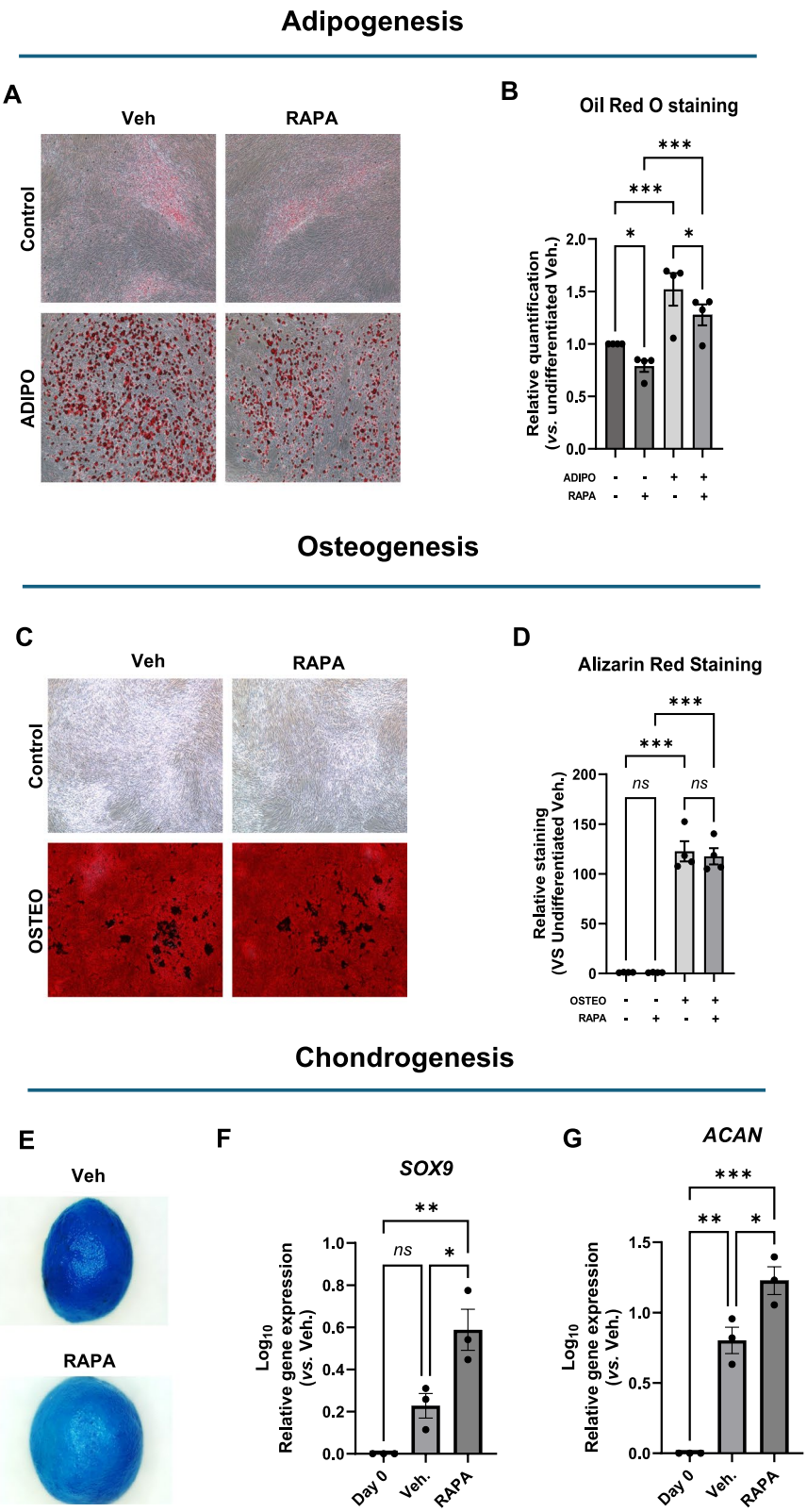

Fig. 2 (See legend on previous page.)

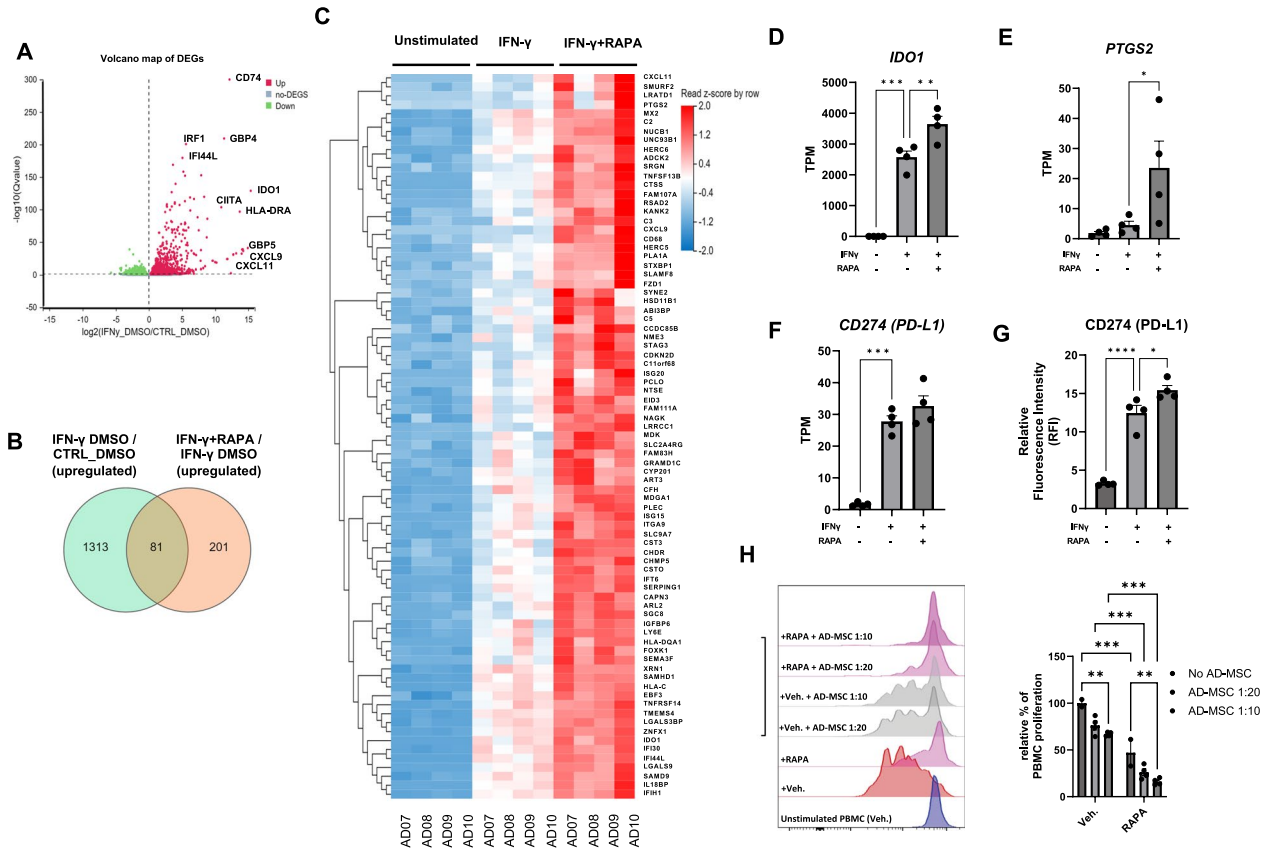

Fig. 3 Rapamycin and AD-MSCs exert additive immunosuppressive effects. The expression profiles of AD-MSCs (n = 4 donors) incubated with 10 nM rapamycin or 0.01% DMSO for 48 h, after IFN-γ stimulation or not, were analyzed by RNA sequencing. Cells (1.5×10^4 cells/cm^2) were cultured for 24 h before treatment. **A** Volcano plot showing all genes upregulated or downregulated by exposure to IFN-γ. **B** Venn diagram showing the genes deregulated by IFN-γ (*vs* CTRL_Veh.) (green circle) and by IFN-γ + RAPA (*vs* IFN-γ) (orange circle) and by both. **C** Heatmap showing the 81 genes deregulated by both IFN-γ and IFN- γ + RAPA. **D**, **E**, **F** Transcripts Per Million (TPM) of *IDO1*, *PTGS2*, and *CD27*. **G** PD-L1 protein overexpression determined by flow cytometry in the indicated conditions. **H** Flow cytometry analysis of the proliferation of PHA-stimulated PBMCs (*vs* Unstimulated) alone or co-cultured with AD-MSCs (1:10 and 1:20 ratio), in the presence of 10 nM rapamycin or vehicle (0.01% DMSO). PBMCs were stained with CellTrace Violet and stimulated with PHA (5 ng/mL) for 4 days. Overlayed histograms (left) and quantification of PBMC proliferation. (right). All error bars represent SEM; *p*-values * < 0.05, ** < 0.01, *** < 0.001 (two-way ANOVA)

IFN-γ vehicle *vs.* Unstimulated vehicle), but its level was not further increased by rapamycin (Fig. 3F). However, when we measured PD-L1 protein expression in AD-MSCs in the same culture condition by flow cytometry, we found that rapamycin further increased its expression compared with IFN-γ alone (Relative Fluorescence Intensity (RFI) = 3.27, 9.52, and 15.41 for unstimulated vehicle, IFN-γ vehicle, and IFN-γ + RAPA, respectively) (Fig. 3G).

Lastly, we tested the AD-MSC functional immunosuppressive properties in co-culture with PHA-stimulated PBMCs (1:20 and 1:10 ratios) in the presence of 10 nM rapamycin or DMSO (control) (Fig. 3H). As expected from previous publications, AD-MSCs reduced PHA-stimulated PBMC proliferation in function of the used ratio (proliferation percentage = 76.16% at 1:20 and 66.87% at 1:10 and thus, 23.84% and 33.13% of relative inhibition, respectively). Rapamycin alone also reduced PBMC proliferation (47.01% of proliferation, and thus 52.99% of relative inhibition). Remarkably, proliferation inhibition was higher in the presence of both rapamycin and AD-MSCs at both ratios (proliferation percentage = 26.06% at 1:20 and 16.05% at 1:10, and thus 73.94% and 83.95% of relative inhibition, respectively).

Rapamycin enhances AD-MSC regenerative properties for the functional rescue of chondrocytes from patients with OA.

To further explore rapamycin potential to improve the AD-MSC regenerative capacities in OA joints, we first defined the gene signature of OA cartilage. To this aim, we reanalyzed a publicly available RNA sequencing dataset (GSE114007) that compared 20 OA and 18 healthy cartilage samples. We identified an OA-associated gene signature that included 1956 upregulated

and 1878 downregulated genes (FDR < 0.05) (data not shown). Analysis of the list of the 1956 upregulated genes with *KEGG Disease* showed that they were perturbed in pathologies of the connective tissues linked to ossification (calcification) and fibrosis (Fig. S4A). Like in the original publication [22], we mapped the whole list of DEGs to *KEGG Pathway* and identified FOXO, PI3K-AKT, HIF-1, circadian rhythm and extracellular matrix-related (protein digestion and absorption, focal adhesion) as significantly affected pathways in OA cartilage (Fig. S4B). This analysis also revealed that Wnt, TNF, Apoptosis and Insulin signaling were deregulated in OA cartilage. Submission of the same DEG list to *REACTOME* revealed a significant impact of OA on extracellular matrix-associated pathways, such as collagen deposition and the TGF-β/SMAD signaling cascade (Fig. S4C). Lastly, in OA cartilage, the classical hypertrophic and bone-associated markers *ALPL, COL10A1, SP7, SPP1,* and *POSTN* were upregulated ($Log_2(FC) = 4.04$, 1,35, 1.55, 2.50, and 5.44, respectively) (Fig. S4D). The *COL1A1, COL3A1, COL5A1,* and *ELN* fibrosis markers also were upregulated ($Log_2(FC) = 5.80$, 2.65, 1.82, 2.26, respectively).

Next, to mimic the conditions of intra-articular co-delivery of rapamycin and GMP-compliant AD-MSCs in OA joints, we set up an in vitro model mimicking clinical trial conditions using Transwell co-cultures of chondrocytes from 3 different OA patients with/without AD-MSCs (Fig. 4A). All combinations mixing each therapeutic cells with each OA chondrocytes culture were tested at 1:7 ratio, in presence or not of 10 nM

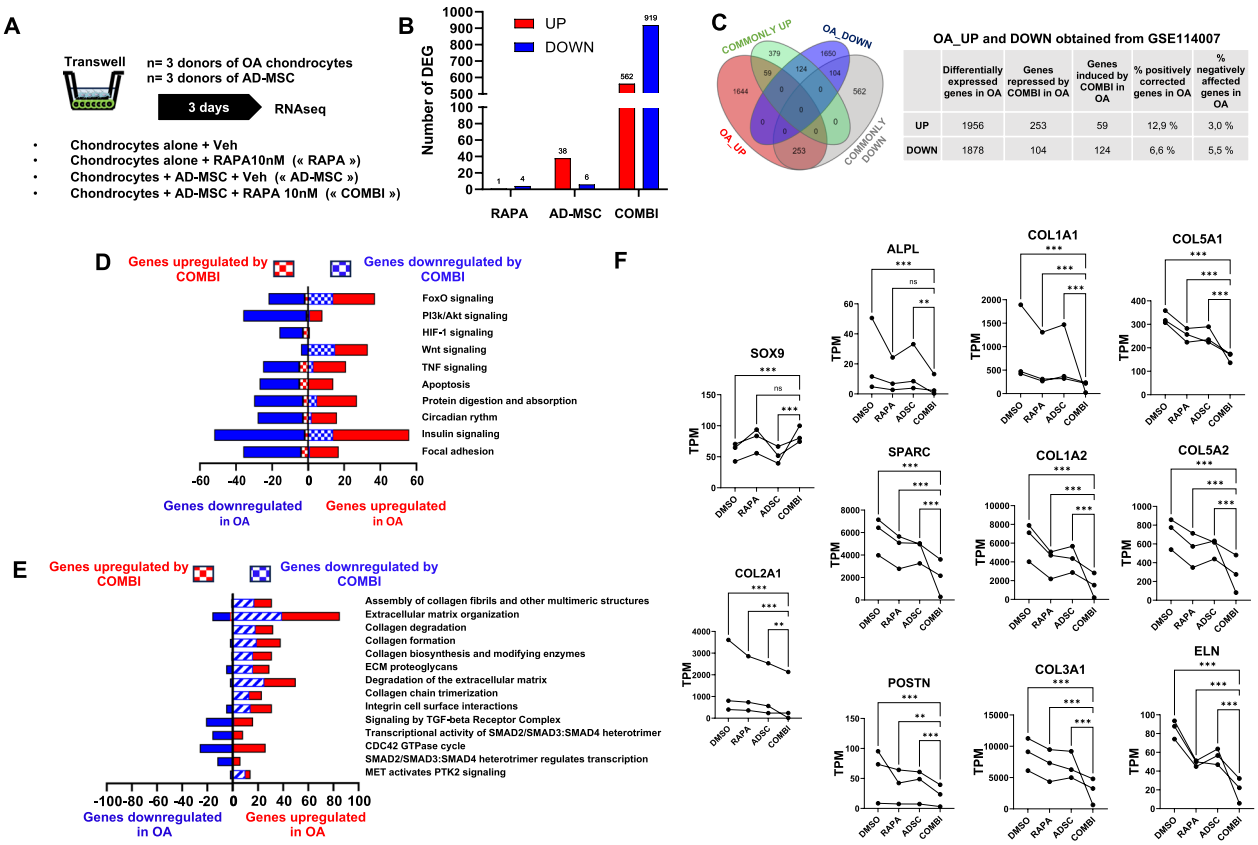

Fig. 4 Improved therapeutic effects of AD-MSCs in the presence of rapamycin on OA chondrocytes. **A** Schematic representation of the experiment design: OA chondrocytes (n = 3 donors) were cultured alone or with AD-MSCs (n = 3 donors) on Transwell inserts, in the presence of 10 nM rapamycin or 0.01% DMSO (vehicle) for 72 h. The comparison groups are indicated below. **B** Histogram showing the number of differentially expressed genes (DEG) in each comparison group relative to DMSO. **C** Venn diagram and the associated chart showing the number of genes modulated by the COMBI condition compared with the OA chondrocyte signature (reanalysis of the GSE114007 dataset in Fig. S4). **D** Histogram showing the *KEGG pathways* significantly deregulated (FDR ≤ 0.05) in OA (from Fig. S4, filled bars) and the effect of COMBI on their expression (dashed bars). **E** Histogram showing the *REACTOME* pathways significantly deregulated (FDR ≤ 0.05) in OA (discovered from the GSE114007 dataset reanalysis) (filled bars) and the effect of COMBI on the same pathways (dashed bars). **F** Line plots showing the Transcripts Per Million (TPM) for chondrogenic (*SOX9*), hypertrophic (*ALPL, SPARC, POSTN*) and fibrosis markers (*COL1A1, COL3A1, COL5A1)* in the indicated conditions; *p*-values: ** < 0.01, *** < 0.001 (two-way ANOVA)

Rapamycin. After 3 days, we isolated total RNA from OA chondrocytes. We excluded two of the 24 samples due to low RNA quality. The comparison groups were as follows: Chondrocytes + RAPA *vs.* Chondrocytes + Vehicle (RAPA hereafter), Chondrocytes + AD-MSC + Vehicle *vs.* Chondrocytes + Vehicle (AD-MSC hereafter) and Chondrocytes + AD-MSC + RAPA *vs.* Chondrocytes + AD-MSC + Vehicle (COMBI hereafter). Only few genes in OA chondrocytes were significantly modulated by rapamycin alone (n = 1 upregulated and n = 4 downregulated) and AD-MSCs alone (n = 38 upregulated and n = 6 downregulated), whereas the combination of rapamycin and AD-MSCs led to significant modulation of 3108 genes (n = 2527 upregulated and n = 581 downregulated) (Fig. 4B). We then analyzed these expression data using a convolution approach to identify genes that were modulated in at least two chondrocyte cultures from different donors co-cultured with AD-MSCs from the three donors. We identified 562 upregulated and 919 downregulated genes. Then, we mapped these gene lists to the OA gene signature previously defined using cartilage samples. Among the 1956 genes overexpressed in OA cartilage (Fig. S4), 253 genes were downregulated in the COMBI condition (12.9% of positive correction) and 59 genes were upregulated (3% of negative correction). Among the 1878 genes downregulated in OA, 124 were induced by the COMBI condition (6.6% of positive correction) and 104 genes were further downregulated (5.5% of negative correction) (Fig. 4C). To highlight COMBI impact on the OA-associated *KEGG* and *REACTOME* pathways, we mapped the DEG list found in COMBI to these databases (Fig. S4B and C) and merged the results on the same histograms as presented on supplementary Fig. 1 (Fig. 4D and E, respectively). Remarkably, COMBI affected the FOXO signaling pathways and extracellular matrix-related organization but not the PI3K and TGFβ pathways at the transcriptomic level.

The RNA sequencing data analysis also showed that COMBI had strong synergetic effects on the OA phenotype by significantly reducing the expression of fibrosis markers (*COL1A1, COL3A1, COL5A1*) and hypertrophic OA markers (*ALPL, SPARC, POSTN*), and by upregulating *SOX9* (chondrogenic markers) in OA chondrocytes compared with AD-MSCs and RAPA alone (Fig. 4F).

Therefore, our findings reveal that the combination of AD-MSCs and rapamycin has a strong anti-fibrotic synergy and a broad impact on the transcriptomic profile of OA chondrocytes toward the healthy cartilage phenotype.

Upon incubation with rapamycin, AD-MSCs overexpress Hedgehog or TGF-β regulatory genes and secrete the pro-survival factor GAS6.

As OA chondrocytes and AD-MSCs were co-cultured using Transwell inserts, the anti-fibrotic and anti-hypertrophic effects observed in OA chondrocytes could only be explained by the secretion of specific factors by AD-MSCs in presence of rapamycin. To identify these secreted factors, we used RNA sequencing to compare gene expression in rapamycin-treated and vehicle-treated AD-MSCs. *KEGG Pathway* analysis of the list of rapamycin-upregulated genes in AD-MSCs showed that the Hedgehog and TGF-β signaling cascades were significantly enriched (Fig. 5A–B). To filter and represent in a heatmap the genes encoding extracellular secreted factors, we used the *Gene Ontology* term *"Extracellular Region"* (GO_C 0005576) for the whole list of DEGs after rapamycin exposure (Fig. 5C). Lastly, we compared the expression profiles for these identified genes in AD-MSCs incubated with rapamycin in the presence or not of IFN-γ to recapitulate the inflammatory microenvironment found in OA joints. Through statistical analysis, we found that genes encoding Hedgehog regulatory factors (*e.g. SCUBE2* [24], *MEGF8* [25]) and TGF-β inhibitory factors (e.g. *FST* [26] and *THSD4* [27]) were significantly upregulated by exposure to rapamycin alone (Fig. 5D). Moreover, the pro-survival factor GAS6 [28] was significantly overexpressed at the gene (Fig. 5E) and protein (Fig. 5F) level in AD-MSCs following rapamycin addition independently of IFN-γ, thus revealing its therapeutic interest.

Discussion

In the past decade, MSCs isolated from different tissues including adipose tissue, bone marrow, umbilical cord and placenta, but also from body fluids (*e.g.* urine, amniotic fluid, or menstrual blood) [29, 30], have attracted considerable interest for therapeutic applications due to their ease of isolation and expansion and their unique properties [1]. Of note, several studies highlighted that MSCs display variable features in function of the cell source [31–33]. On the basis of their ability to differentiate into different cell types and their immunomodulatory effects, MSC-based therapies have been tested in clinical trials for the treatment of degenerative diseases, including OA. However, achieving the desired results has been challenging for clinicians [9].

As senescent cells are implicated in many degenerative diseases, including OA, researchers have focused on targeting their detrimental effects on the surrounding tissues to enhance MSC therapeutic efficacy [34]. On the other hand, senescent MSCs could hamper tissue repair

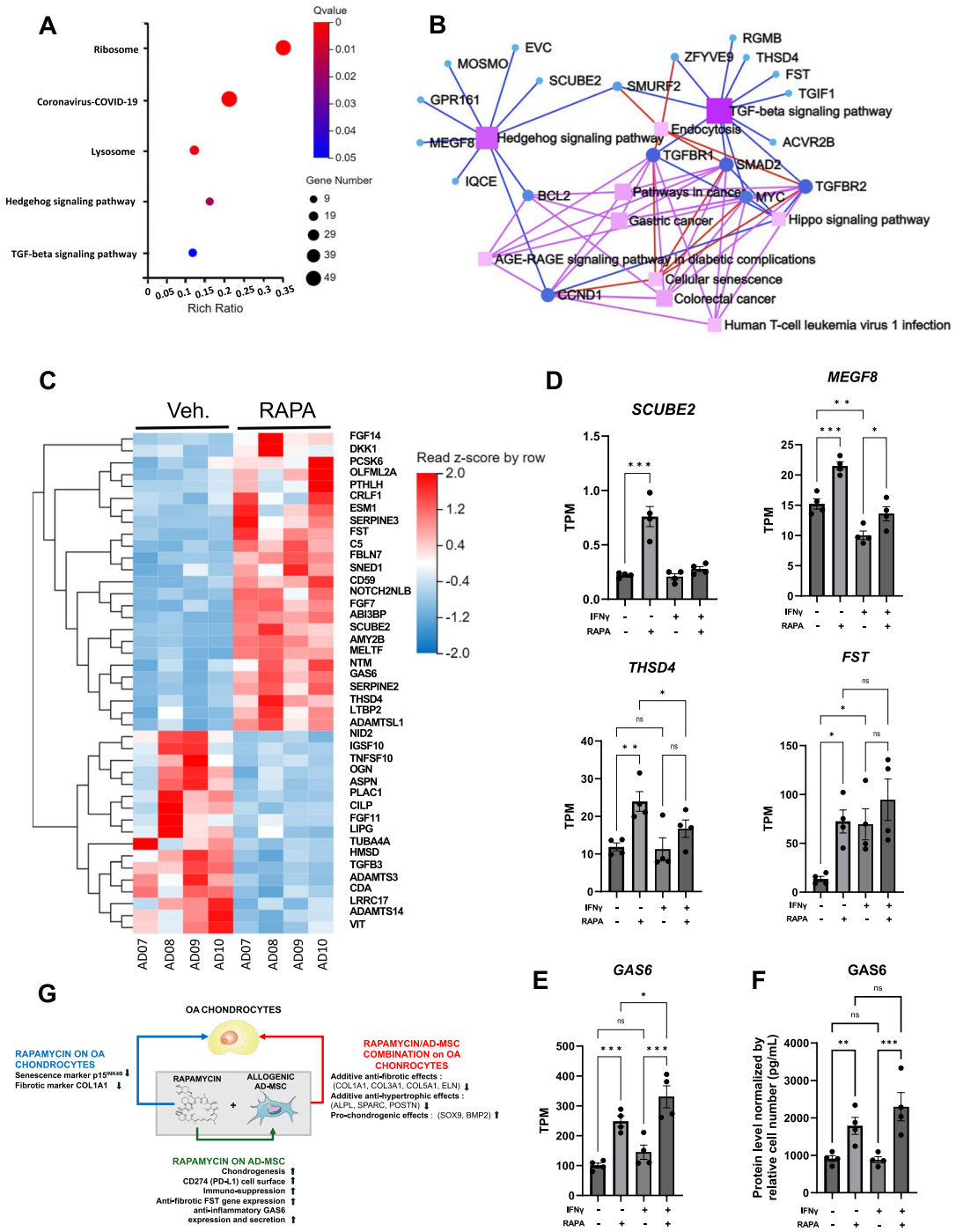

Fig. 5 Rapamycin induces the secretion of chondroprotective and regenerative factors by AD-MSCs. **A** The list of rapamycin-upregulated genes (*vs* vehicle) in AD-MSCs was submitted to *KEGG Pathway*. Significantly affected pathways (at FDR ≤ 0.05) were plotted as a bubble chart. **B** The *KEGG network* of "Hedgehog signaling" and "TGF-β signaling" upregulated genes identified in panel A. **C** Genes encoding extracellular factors and upregulated or downregulated in AD-MSCs were selected using the *Gene Ontology* term *"Extracellular region"* (GO0005576) and plotted as a Z-score heatmap of normalized counts showing the vehicle- *vs.* rapamycin-treated groups. **D** Transcripts Per Million (TPM) of extracellular factors from the "Hedgehog signaling" *(SCUBE2* and *MEGF8*) and "TGF-β signaling" (*LTBP2* and *FST*) pathways were extracted and plotted as dot-histograms to show their relative expression in the indicated conditions. **E** TPM of the pro-regenerative factor *GAS6*. **F** GAS6 secreted by AD-MSCs upon exposure to rapamycin or/and IFN-γ. GAS6 level in supernatants was quantified by ELISA and normalized to the relative number of cells; **G** Diagram summary of all results. *p*-values: * < 0.05, ** < 0.01, *** < 0.001 (two-way ANOVA)

and mediate senescence-associated secretory phenotypes that affect the surrounding microenvironment [35]. Consequently, priming MSCs with senescence-targeting drugs, such as metformin or fisetin, has emerged as a promising strategy to improve their efficacy in OA and other degenerative diseases [36, 37].

Rapamycin, the first clinically-approved mTOR inhibitor, is prescribed in several immune disorders, including organ transplant rejection, due to its ability to modulate the immune response and reduce inflammation [38]. Indeed, rapamycin inhibition of T-cell proliferation, B-cell differentiation and antibody production contributes to its immunosuppressive effects [38]. Recently, it has been also shown that rapamycin slows down cellular senescence and the associated fibrosis in various conditions [39]. Here, we confirmed that rapamycin reduces senescence/fibrotic marker expression in freshly isolated OA chondrocytes. Therefore, rapamycin is an interesting candidate to prevent the negative bystander effects of joint senescence on therapeutic cells (Fig. 1).

We then showed that AD-MSC regenerative properties can be improved when they are combined with rapamycin. Indeed, rapamycin promoted chondrogenic markers in AD-MSCs differentiated into chondrocytes, the only cell type present in cartilage (Fig. 2). We also revealed rapamycin additive effects on AD-MSC immunomodulatory capacities, which could contribute to reduce joint inflammation. Moreover, AD-MSCs were sensitized to the inflammatory microenvironment in the presence of rapamycin, leading to the upregulation of genes encoding immunosuppressive molecules, such as *IDO1* and *PTGS2,* and the cell surface PD-L1, an immune checkpoint component. Accordingly, in the presence of rapamycin, AD-MSCs reduced more efficiently PBMC proliferation induced by PHA stimulation (Fig. 3). This additive effect was not expected and as AD-MSC immunosuppressive properties are mainly dependent on their metabolic status [40], it would be interesting to determine whether rapamycin can reprogram AD-MSC metabolism to sensitive these cells to inflammation.

Using RNA sequencing, we showed that the combination of AD-MSCs + rapamycin (COMBI) had strong synergetic regenerative effects on the phenotype of OA chondrocytes compared with AD-MSCs and rapamycin alone (Fig. 4). Mechanistically, we found that in the presence of rapamycin, AD-MSCs strongly expressed gene encoding several developmental Hedgehog (*SCUBE2*, *MEGF8)* and TGF-β regulatory factors (*FST*, *THSD4*). These findings are particularly important with regard to the *FST* and *THSD4* genes, which encode TGF-β inhibitory factors that could potentially contribute to a reduction in the excess and, consequently, the deleterious level of TGF-β family members in the degenerated joint [41]. Moreover, secretion by AD-MSCs of the mitotic and pro-survival factor GAS6 was increased (Fig. 5), independently of the inflammatory context [42]. GAS6 binds to AXL family receptors and modulates the inflammatory response during tissue repair by inhibiting the release of pro-inflammatory cytokines [43]. Moreover, GAS6 displays anti-inflammatory effects on synoviocytes isolated from patients with OA [44] and has been identified as one of the factors implicated the OA protection of MLR mice [45]. Therefore, we propose that in the presence of rapamycin and in an inflammatory microenvironment, GAS6 secreted by AD-MSCs could contribute to improve AD-MSC effects on OA chondrocytes. More in vitro studies are needed to confirm this hypothesis.

Before using rapamycin for OA patients, further limits must be considered. Several trials in OA targeting inflammatory mediators using anti-cytokine therapy were disappointing [46]. It is now widely accepted that the main MSC therapeutic effects are mediated primarily through the short-term secretion of trophic factors that reduce inflammation and modulate immune cells [47]. However, a recent well-done large randomized trial demonstrates that current cell therapy approaches in the treatment of OA have variable outcomes and are not notably different from simply treating with corticosteroids [48]. Thus, it is critical to evaluate the efficacy of rapamycin in human OA patients to determine whether the additive in vitro effect results in greater clinical benefit than MSC-based strategy. In addition, it would be important to verify after intra-articular injection, that the residual amount of rapamycin in the bloodstream of the treated patient will not induce systemic immunosuppression. Finally, the co-culture conditions of the AD-MSC-rapamycin combination could also be replicated this time with cartilage explants in the presence of joint fluid from OA patients to better approximate human pathological conditions.

To conclude, this study proposes that rapamycin, a clinically approved molecule, holds promise as adjuvant to enhance stem cell-based therapeutic efficacy in senescence-driven OA (Fig. 5). However, these results need to be investigated in a robust randomized clinical trial.

Supplementary Information

The online version contains supplementary material available at https://doi.org/10.1186/s13287-024-04090-8.

Additional file 1.

Acknowledgements

We deeply thank (1) the Orthopedic department directed by Prof Louis Dagneaux; (2) Dr Rosanna Ferreira-Lopez, Sophie Grasset and Prof Yves-Marie Pers from the Rheumatology department at CHU Lapeyronie, Montpellier, France, for providing clinical data and patient signed consents; (3) The ECELL-FRANCE clinical and pre-clinical platform at Montpellier University, France, for their help in setting up the flow cytometry analysis; (4) Cartigen facilities,

Montpellier Hospital, France, for their help in confocal microscopy analysis; (5) the Montpellier Ressources Imagerie (MRI) for cytometry facilities. Some grammatical English sentence corrections were done with the help of on-line correctors.

Author contributions
Experimental design, analysis and interpretations: DV, GT, EP, AC, MF, CG, JMB. Patient cohort management, consents and surgery: YMP, RFL, LD and CJ. Study management and financial support: CG, CJ and JMB. Manuscript writing, critical reading, correction and submission: DV, GT, YMP, LD, CJ, CG and JMB.

Funding
D.V was a PhD student with an ANRT/Cifre studentship with MedXCell/Montpellier Life Science (Montpellier, France). This work was supported by Graine Academic/private fellowship from Region Occitanie, France awarded to JMB.

Availability of data and materials
RNA-seq data obtained in this study are available online: ArrayExpress accession: E-MTAB-14215 for AD-MSCs and E-MTAB-14216 for chondrocytes co-cultivated with AD-MSCs.

Declarations

Ethics approval and Consent to participate
Informed consent was obtained from all subjects involved in the study. The study was conducted in accordance with the Declaration of Helsinki and approved by (1) the Regional Investigational Review Board "Comité de Protection des Personnes SUDEST II, Lyon, France" (Protocol 2019-A01067-50 approved on September 11th, 2019) and (2) Regional Investigation Review board Montpellier (number approval IRB-MTP_2022_11_202201238). IRB Accreditation number: 198711 under the title: Consolidation of biological collections with a view to a harmonized approach to research into rheumatological diseases and approved on November 28, 2022.

Consent for publication
All authors agree to publish this version of the article.

Artificial intelligence
The authors declare that they have not used Artificial Intelligence in this study.

Competing interests
None.

Author details
[1]IRMB, Univ Montpellier, INSERM, CHU St Eloi, 80 AV A Fliche, 34295-Cedex-05 Montpellier, France. [2]MedXCell, IRMB, CHU St Eloi, Cyborg, Montpellier, France. [3]Clinical Immunology and Osteoarticular Diseases Therapeutic Unit, Hôpital Lapeyronie, Montpellier, France. [4]Present Address: Rheumatology department, Regional Narbonne Hospital, Narbonne, France. [5]Hôpital Lapeyronie, Orthopedic Service, Montpellier, France.

Received: 5 July 2024 Accepted: 3 December 2024
Published online: 15 January 2025

References

1. Maldonado VV, Patel NH, Smith EE, Barnes CL, Gustafson MP, Rao RR, et al. Clinical utility of mesenchymal stem/stromal cells in regenerative medicine and cellular therapy. J Biol Eng. 2023;17(1):44.
2. Margiana R, Markov A, Zekiy AO, Hamza MU, Al-Dabbagh KA, Al-Zubaidi SH, et al. Clinical application of mesenchymal stem cell in regenerative medicine: a narrative review. Stem Cell Res Ther. 2022;13(1):366.
3. Bunnell BA. Adipose tissue-derived mesenchymal stem cells. Cells. 2021;10(12):3433.
4. Gao Q, Wang L, Wang S, Huang B, Jing Y, Su J. Bone marrow mesenchymal stromal cells: identification, classification, and differentiation. Front Cell Dev Biol. 2022;3(9): 787118.
5. Semenova E, Grudniak MP, Machaj EK, Bocian K, Chroscinska-Krawczyk M, Trochonowicz M, et al. Mesenchymal stromal cells from different parts of umbilical cord: approach to comparison and characteristics. Stem Cell Rev Rep. 2021;17(5):1780–95.
6. Renesme L, Pierro M, Cobey KD, Mital R, Nangle K, Shorr R, et al. Definition and characteristics of mesenchymal stromal cells in preclinical and clinical studies: a scoping review. Stem Cells Transl Med. 2022;11(1):44–54.
7. Müller L, Tunger A, Wobus M, Von Bonin M, Towers R, Bornhäuser M, et al. Immunomodulatory properties of mesenchymal stromal cells: an update. Front Cell Dev Biol. 2021;9(9): 637725.
8. Kabat M, Bobkov I, Kumar S, Grumet M. Trends in mesenchymal stem cell clinical trials 2004–2018: Is efficacy optimal in a narrow dose range? STEM CELLS Transl Med. 2020;9(1):17–27.
9. Du X, Liu Z, Tao X, Mei Y, Zhou D, Cheng K, et al. Research progress on the pathogenesis of knee osteoarthritis. Orthop Surg. 2023;15(9):2213–24.
10. Liu Y, Zhang Z, Li T, Xu H, Zhang H. Senescence in osteoarthritis: from mechanism to potential treatment. Arthritis Res Ther. 2022;24(1):174.
11. Du X, Cai L, Xie J, Zhou X. The role of TGF-beta3 in cartilage development and osteoarthritis. Bone Res. 2023;11(1):2.
12. Pers YM, Rackwitz L, Ferreira R, Pullig O, Delfour C, Barry F, et al. Adipose mesenchymal stromal cell-based therapy for severe osteoarthritis of the knee: a phase i dose-escalation trial: ASCs for severe OA of the knee. STEM CELLS Transl Med. 2016;5(7):847–56.
13. Sadeghirad B, Rehman Y, Khosravirad A, Sofi-Mahmudi A, Zandieh S, Jomy J, Patel M, Couban RJ, Momenilandi F, Burnham R, Poolman RW, Busse JW. Mesenchymal stem cells for chronic knee pain secondary to osteoarthritis: a systematic review and meta-analysis of randomized trials. Osteoarthritis Cartilage. 2024;32(10):1207–19. https://doi.org/10.1016/j.joca.2024.04.021.
14. Moeinabadi-Bidgoli K, Mazloomnejad R, Beheshti Maal A, Asadzadeh Aghdaei H, Kazem Arki M, Hossein-Khannazer N, et al. Genetic modification and preconditioning strategies to enhance functionality of mesenchymal stromal cells: a clinical perspective. Expert Opin Biol Ther. 2023;23(6):461–78.
15. Ganesh SK, Subathra DC. Molecular and therapeutic insights of rapamycin: a multi-faceted drug from streptomyces hygroscopicus. Mol Biol Rep. 2023;50(4):3815–33.
16. Mannick JB, Lamming DW. Targeting the biology of aging with mTOR inhibitors. Nat Aging. 2023;3(6):642–60.
17. Zhang L, Pitcher LE, Prahalad V, Niedernhofer LJ, Robbins PD. Targeting cellular senescence with senotherapeutics: senolytics and senomorphics. FEBS J. 2023;290(5):1362–83.
18. Kastrup J, Haack-Sørensen M, Juhl M, Harary Søndergaard R, Follin B, Drozd Lund L, et al. Cryopreserved off-the-shelf allogeneic adipose-derived stromal cells for therapy in patients with ischemic heart disease and heart failure-a safety study: allogeneic ASC therapy in heart failure. STEM CELLS Transl Med. 2017;6(11):1963–71.
19. Tejedor G, Boisguerin P, Vivès É, Jorgensen C, Guicheux J, Vinatier C, Gondeau C, Djouad F. PPARβ/δ-interfering peptide enhanced mesenchymal stromal cell immunoregulatory properties. Stem Cells Int. 2022;2022:1–12. https://doi.org/10.1155/2022/5494749.
20. Malaise O, Tachikart Y, Constantinides M, Mumme M, Ferreira-Lopez R, Noack S, et al. Mesenchymal stem cell senescence alleviates their intrinsic and seno-suppressive paracrine properties contributing to osteoarthritis development. Aging. 2019;11(20):9128–46.
21. Maumus M, Manferdini C, Toupet K, Peyrafitte JA, Ferreira R, Facchini A, et al. Adipose mesenchymal stem cells protect chondrocytes from degeneration associated with osteoarthritis. Stem Cell Res. 2013;11(2):834–44.
22. Fisch KM, Gamini R, Alvarez-Garcia O, Akagi R, Saito M, Muramatsu Y, et al. Identification of transcription factors responsible for dysregulated networks in human osteoarthritis cartilage by global gene expression analysis. Osteoarthritis Cartilage. 2018;26(11):1531–8.
23. de Noronha N, Mizukami A, Caliári-Oliveira C, Cominal JG, Rocha JLM, Covas DT, et al. Priming approaches to improve the efficacy of mesenchymal stromal cell-based therapies. Stem Cell Res Ther. 2019. https://doi.org/10.1186/s13287-019-1224-y.
24. Lin YC, Roffler SR, Yan YT, Yang RB. Disruption of *Scube2* impairs endochondral bone formation. J Bone Miner Res. 2015;30(7):1255–67.

25. Kong JH, Young CB, Pusapati GV, Patel CB, Ho S, Krishnan A, et al. A membrane-tethered ubiquitination pathway regulates hedgehog signaling and heart development. Dev Cell. 2020;55(4):432-49.e12.
26. Walpurgis K, Weigand T, Knoop A, Thomas A, Reichel C, Dellanna F, et al. Detection of follistatin-based inhibitors of the TGF-β signaling pathways in serum/plasma by means of LC-HRMS/MS and Western blotting. Drug Test Anal. 2020;12(11–12):1636–48.
27. Liu J, Huang Z, Chen HN, Qin S, Chen Y, Jiang J, et al. ZNF37A promotes tumor metastasis through transcriptional control of THSD4/TGF-β axis in colorectal cancer. Oncogene. 2021;40(19):3394–407.
28. Di Stasi R, De Rosa L, D'Andrea LD. Therapeutic aspects of the Axl/Gas6 molecular system. Drug Discov Today. 2020;25(12):2130–48.
29. Huang RL, Li Q, Ma JX, Atala A, Zhang Y. Body fluid-derived stem cells—an untapped stem cell source in genitourinary regeneration. Nat Rev Urol. 2023;20(12):739–61.
30. Chen L, Huang Y, Zhang N, Qu J, Fang Y, Fu J, et al. Single-cell RNA sequencing reveals reduced intercellular adhesion molecule crosstalk between activated hepatic stellate cells and neutrophils alleviating liver fibrosis in hepatitis B virus transgenic mice post menstrual blood-derived mesenchymal stem cell transplantation. MedComm. 2024;5(8): e654.
31. Chen R, Xie Y, Zhong X, Chen F, Gong Y, Wang N, et al. MSCs derived from amniotic fluid and umbilical cord require different administration schemes and exert different curative effects on different tissues in rats with CLP-induced sepsis. Stem Cell Res Ther. 2021;12(1):164.
32. Gou Y, Huang Y, Luo W, Li Y, Zhao P, Zhong J, et al. Adipose-derived mesenchymal stem cells (MSCs) are a superior cell source for bone tissue engineering. Bioact Mater. 2024;34:51–63.
33. Brown C, McKee C, Bakshi S, Walker K, Hakman E, Halassy S, et al. Mesenchymal stem cells: cell therapy and regeneration potential. J Tissue Eng Regen Med. 2019;13(9):1738–55.
34. Cao X, Luo P, Huang J, Liang C, He J, Wang Z, et al. Intraarticular senescent chondrocytes impair the cartilage regeneration capacity of mesenchymal stem cells. Stem Cell Res Ther. 2019;10(1):86.
35. Jiang X, Li W, Ge L, Lu M. Mesenchymal stem cell senescence during aging: from mechanisms to rejuvenation strategies. Aging Dis. 2023;14(5):1651.
36. Mullen M, Nelson AL, Goff A, Billings J, Kloser H, Huard C, et al. Fisetin attenuates cellular senescence accumulation during culture expansion of human adipose-derived stem cells. Stem Cells. 2023;41(7):698–710.
37. Park MJ, Moon SJ, Baek JA, Lee EJ, Jung KA, Kim EK, et al. Metformin augments anti-inflammatory and chondroprotective properties of mesenchymal stem cells in experimental osteoarthritis. J Immunol. 2019;203(1):127–36.
38. Sehgal SN. Sirolimus: its discovery, biological properties, and mechanism of action. Transplant Proc. 2003;35(3):S7-14.
39. Fu W, Wu G. Targeting mTOR for anti-aging and anti-cancer therapy. Molecules. 2023;28(7):3157.
40. Contreras-Lopez RA, Elizondo-Vega R, Torres MJ, Vega-Letter AM, Luque-Campos N, Paredes-Martinez MJ, et al. PPARβ/δ-dependent MSC metabolism determines their immunoregulatory properties. Sci Rep. 2020;10(1):11423.
41. Zhen G, Wen C, Jia X, Li Y, Crane JL, Mears SC, et al. Inhibition of TGF-β signaling in mesenchymal stem cells of subchondral bone attenuates osteoarthritis. Nat Med. 2013;19(6):704–12.
42. Goruppi S, Ruaro E, Schneider C. Gas6, the ligand of Axl tyrosine kinase receptor, has mitogenic and survival activities for serum starved NIH3T3 fibroblasts. Oncogene. 1996;12(3):471–80.
43. Bellan M, Cittone MG, Tonello S, Rigamonti C, Castello LM, Gavelli F, et al. Gas6/TAM System: a key modulator of the interplay between inflammation and fibrosis. Int J Mol Sci. 2019;20(20):5070.
44. Vago JP, Valdrighi N, Blaney-Davidson EN, Hornikx DLAH, Neefjes M, Barba-Sarasua ME, et al. Gas6/Axl axis activation dampens the inflammatory response in osteoarthritic fibroblast-like synoviocytes and synovial explants. Pharmaceuticals. 2023;16(5):703.
45. Tejedor G, Luz-Crawford P, Barthelaix A, Toupet K, Roudières S, Autelitano F, et al. MANF produced by MRL mouse-derived mesenchymal stem cells is pro-regenerative and protects from osteoarthritis. Front Cell Dev Biol. 2021;9: 579951.
46. Chevalier X, Eymard F, Richette P. Biologic agents in osteoarthritis: hopes and disappointments. Nat Rev Rheumatol. 2013;9(7):400–10.
47. Pers YM, Quentin J, Feirreira R, Espinoza F, Abdellaoui N, Erkilic N, et al. Injection of adipose-derived stromal cells in the knee of patients with severe osteoarthritis has a systemic effect and promotes an anti-inflammatory phenotype of circulating immune cells. Theranostics. 2018;8(20):5519–28.
48. Mautner K, Gottschalk M, Boden SD, Akard A, Bae WC, Black L, et al. Cell-based versus corticosteroid injections for knee pain in osteoarthritis: a randomized phase 3 trial. Nat Med. 2023;29(12):3120–6.

Publisher's Note